J. Dairy Sci. 104:2529–2538
https://doi.org/10.3168/jds.2020-19500

Ultrasensitive and simultaneous detection of 6 nonsteroidal anti-inflammatory drugs by colloidal gold strip sensor

Lu Lin,[1,2] Liguang Xu,[1,2] Hua Kuang,[1,2] Jing Xiao,[3]* and Chuanlai Xu[1,2]*
[1]State Key Laboratory of Food Science and Technology, Jiangnan University, Wuxi 214121, People's Republic of China
[2]International Joint Research Laboratory for Biointerface and Biodetection, and School of Food Science and Technology, Jiangnan University, Wuxi 214121, People's Republic of China
[3]NHC Key Laboratory of Food Safety Risk Assessment, China National Center for Food Safety Risk Assessment, Beijing 100022, People's Republic of China

ABSTRACT

In this work, an oxicam group–selective monoclonal antibody against 6 nonsteroidal anti-inflammatory drugs (NSAID; meloxicam, lornoxicam, piroxicam, sudoxicam, droxicam, and tenoxicam) was prepared. Also, a spacer arm with carboxyl group was derived at the hydroxyl of meloxicam to generate the meloxicam hapten. The half-maximal inhibitory concentrations (IC_{50}) were, respectively, 0.31 ng/mL for meloxicam, 0.49 ng/mL for lornoxicam, 2.90 ng/mL for piroxicam, 1.95 ng/mL for sudoxicam, 3.08 ng/mL for droxicam, and 5.36 ng/mL for tenoxicam. A colloidal gold immunochromatographic strip based on the monoclonal antibody was developed for the detection of these 6 NSAID in milk. The results could be obtained by the naked eye in 10 min, and the cut-off values and the visual limits of detection in real samples were 5, 5, 10, 10, 25, and 25 ng/mL, and 0.25, 1, 0.5, 0.5, 1, and 1 ng/mL, respectively. This immunochromatopgraphic strip is a suitable tool for on-site detection and screening of oxicam NSAID in milk samples.

Key words: nonsteroidal anti-inflammatory drug, monoclonal antibody, oxicam group selective, cross reaction, immunochromatographic strip

INTRODUCTION

With the continuous increase in requirements of the public for better quality of life, the demand for milk is increasing. As a result, the scale of cattle breeding is expanding, and the risk of disease is also higher. Mastitis (Bertoni et al., 2015) is a common and important disease of dairy cattle, which is one of the main factors limiting the output of milk. Mastitis (Bradley, 2002) refers to the inflammatory response of udder tissue after the invasion of pathogenic bacteria. Meloxicam (**MELO**) is a nonsteroidal anti-inflammatory drug (**NSAID**; Bartos et al., 2019; Woodland et al., 2019), and studies have shown that MELO blocks the synthesis of prostaglandins by inhibiting cyclooxygenase, especially type II cyclooxygenase (Newby et al., 2014; Olson et al., 2016; Pascottini et al., 2019), and ultimately inhibits inflammation. Meloxicam was developed by Germany's Boehringer Ingelheim and has been approved for use in dairy cattle in many European countries to treat mastitis (Swartz et al., 2018) and rapidly resolve inflammation (Newby et al., 2013; Colditz et al., 2019; Shock et al., 2019). During treatment, if the drug is used inappropriately or the withdrawal period for milk is inadequate, it can result in drug residues in milk, which might be a threat to human health. Therefore, the ministry of agriculture and rural affairs of the People's Republic of China have stipulated maximum residue limits for MELO in cattle muscle, liver, and milk of 20, 65, and 15 μg/kg, respectively. In addition, 5 other NSAID of the oxicam group (Figure 1), lornoxicam (**LORN**; Zangaro et al., 2019), piroxicam (**PIRO**; Kazemi et al., 2019), sudoxicam (**SUDO**; Barnette et al., 2020), droxicam (**DRO**; Barnette, et al., 2020), and tenoxicam (**TENO**; You et al., 2018), are also likely to be used in the treatment of cow mastitis because of their anti-inflammatory effects. Consequently, an effective and rapid method for the detection of MELO residues in milk is needed to ensure milk quality and safety.

Several analysis methods have been used to detect the above oxicam group NSAID, such as liquid chromatography–mass spectrometry (**LC-MS**; Rúbies et al., 2016), high-performance thin layer chromatography (Rúbies et al., 2016), HPLC (Kimble et al., 2013; Cox et al., 2014; Emara et al., 2016), and liquid chromatography–tandem mass spectrometry (**LC-MS/MS**; Dowling and Malone, 2011; Shirako al., 2013; Calvo et al., 2016). However, all of these methods need detailed

Received August 20, 2020.
Accepted October 26, 2020.
*Corresponding authors: xiaojing@cfsa.net.cn and xcl@jiangnan.edu.cn

sample pretreatment, expensive instruments, and specially trained professionals. Therefore, these methods are not suitable for on-site detection of large quantities of samples, which limits their popularization and application.

The immunochromatographic strip (**ICS**) is a widely used immunoassay method that has the advantage of short analysis time (results can be obtained in 10 min by the naked eye) as well as being easy to perform and evaluate. According to previous reports, the ICS is widely used for detecting various food hazard factors, including pesticides, antibiotics, biotoxins, and hormones (Hua et al., 2015; Liu et al., 2016; Fang et al., 2019; Majdinasab et al., 2019). At present, no relevant studies have reported determination of NSAID of the oxicam group by ICS. Therefore, a mAb against 6 NSAID of the oxicam group was prepared in this study. Furthermore, the mAb was used to create an ICS to detect 6 NSAID of the oxicam group in milk.

MATERIALS AND METHODS

Materials

The NSAIDs MELO, LORN, PIRO, SUDO, DRO, and TENO were all purchased from J&K Scientific Ltd. (Shanghai, China). Keyhole limpet hemocyanin (**KLH**), ovalbumin (**OVA**), *N*-hydroxysuccinimide, 1-ethyl-3-(3-dimethyl-aminopropyl) carbodiimide, Freund's complete adjuvant, and Freund's incomplete adjuvant were obtained from Sigma-Aldrich Trade Co. Ltd. (Shanghai, China). Polyethylene glycol (**PEG**), RPMI 1640 medium, HAT (hypoxanthine-aminopterin-thymidine) supplement (50×), HT (hypoxanthine-thymidine) supplement (100×), and fetal bovine serum were purchased from Thermo Fisher Scientific Co. Ltd. (Shanghai, China).

Materials used for the ICS, including glass fiber membrane CB-SB08, absorbent pad SX18, and polyvinyl chloride sheet were purchased from Goldbio Tech Co., Ltd. (Shanghai, China). The nitrocellulose membrane Pura-bind RP was purchased from Whatman-Xinhua Filter Paper Co., Ltd. (Hangzhou, China).

Derivation of Hapten

The synthesis steps for the hapten are shown in Figure 2. A solution of MELO (1.00 g) in MeOH (10 mL) was added to 0.16 g of MeONa and stirred at 65°C overnight. The mixture was concentrated to obtain compound 2 as a white solid. Next, 1.20 g of compound 2 in *N*,*N*-dimethylformamide (**DMF**; 30 mL) was added to ethyl 4-bromobutanoate and stirred at 80°C overnight. The mixture was concentrated, and the residue was purified using a silica column to give compound 3 as a yellow solid. Next, 0.80 g of compound 3 was weighed into 4 mL of tetrahydrofuran (THF) in water (3:1, vol/vol), and 0.18 g of $LiOH{\cdot}H_2O$ was added and stirred at room temperature overnight. Then, 2.0 mol/L HCl was added dropwise to the stirring solution until the pH reached 4.0 to 6.0. The aqueous layer was extracted with ethylamine. The combined organic lay-

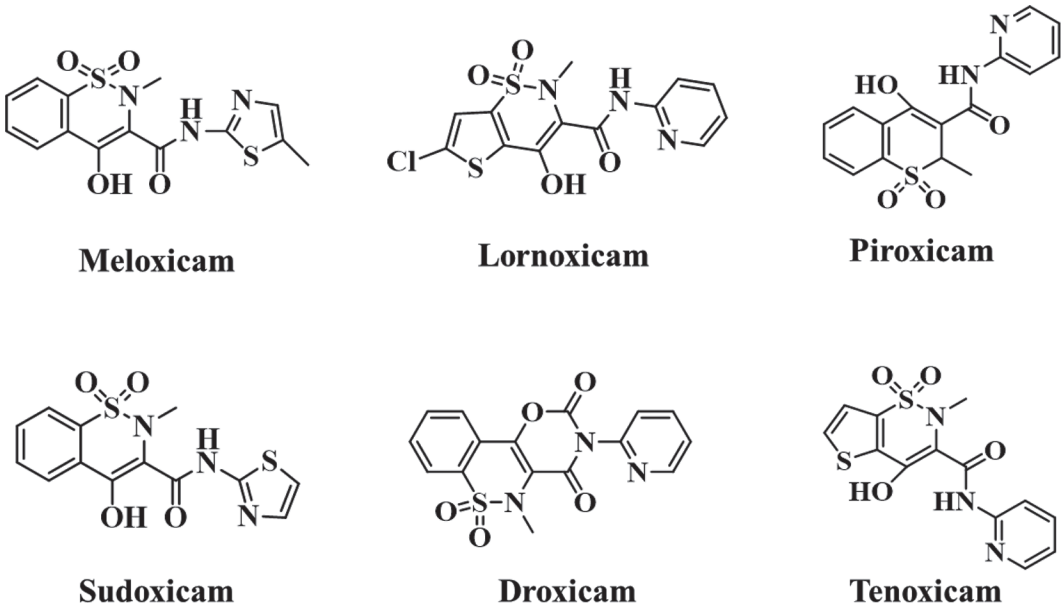

Figure 1. Chemical structures of nonsteroidal anti-inflammatory drugs.

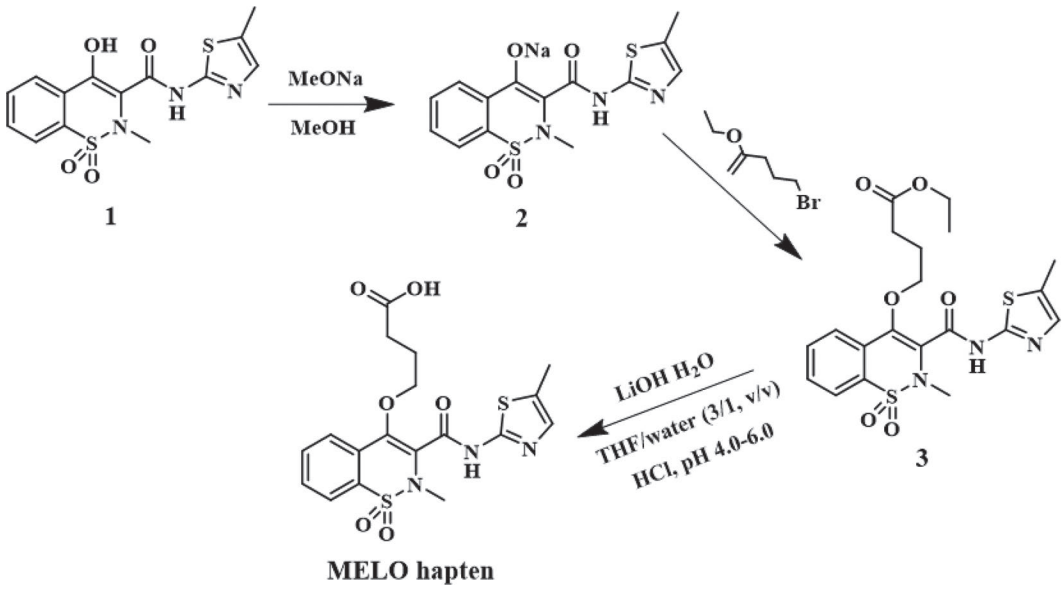

Figure 2. Synthesis of the meloxicam (MELO) hapten. MeOH = methanol, MeONa = sodium methoxide; THF = tetrahydrofuran.

ers were washed with brine, dried over Na_2SO_4, and concentrated to yield the compound MELO hapten as a yellow solid.

Synthesis of Conjugates

The conjugates were both synthesized by the carbodiimide method as described previously (Guo et al., 2016; Wang et al., 2018b). The MELO hapten was coupled to KLH (MELO hapten-KLH) as immunogen, and coupled with OVA (MELO hapten-OVA) as coating antigen. Briefly, 1.7 mg of MELO hapten was dissolved in 260 μL of DMF, and then 2.3 mg of 1-ethyl-3-(3-dimethylaminopropyl) carbodiimide was dissolved in 20 μL of MES. Next, 1.4 mg of *N*-hydroxysuccinimide in 40 μL of DMF was added to the above solution. The mixture was stirred at room temperature for 6 h, then slowly added dropwise to 10 mg of KLH dissolved in 3 mL of 0.01 mol/L borate saline buffer (pH 8.8), and stirred overnight. The reaction solution was dialyzed with 0.01 mol/L phosphate buffer (pH 7.4) for 3 d and stored at −20°C for use. The synthesis of MELO hapten-OVA was similar to the process described above. All conjugates were characterized by UV-visible spectroscopy.

Preparation of the Monoclonal Antibody

All animal studies were performed according to institutional ethical guidelines and were approved by the Committee on Animal Welfare of Jiangnan University. The animal welfare and ethics audit number was JN.No20180930b1001220 [205].

Five female BALB/c mice (8 wk old) were immunized with MELO hapten-KLH by subcutaneous injection into the neck and back. The process of immunization followed that used in previous research (Bolarinwa et al., 2014; Dong et al., 2018; Wang et al., 2019). In brief, for the first immunization, the mice were immunized with 100 μg of Freund's complete adjuvant emulsified with an equal volume of MELO hapten-KLH. Every fourth week, booster immunization was performed with Freund′s incomplete adjuvant mixed with an equal volume of MELO hapten-KLH. The dose of the booster immunization was half that of the first immunization. After the second booster immunization, the antiserum was collected and analyzed by indirect competitive ELISA (**ic-ELISA**). After several booster immunizations, the mouse with the highest titer and inhibition was selected for cell fusion. Three days before cell fusion, the mouse was injected with 25 μg of MELO hapten-KLH by intraperitoneal injection.

Cell fusion was carried out in reference to a previously-described process (Wang et al., 2015, 2016). The spleen cells and the mouse myeloma cells SP2/0 were fused using PEG 1450. The fused cells were cultured in 96-well cell culture plates with HAT selective medium [RPMI 1640 medium containing 10% fetal bovine serum (vol/vol), 10,000 U/mL penicillin, 10,000 μg/mL streptomycin, and 2% HAT (vol/vol)]. The positive hybridomas were screened by ic-ELISA and subcloned 3 times by limiting dilution. The positive hybridomas stably secreting mAb were selected and expanded in culture. Mice were injected with hybridomas for preparation of large amounts of ascites. Finally, the ascites

were purified by protein G affinity chromatography, and the mAb was obtained then stored at −20°C until use.

Characterization of the mAb

The subclass of the mAb was determined by a mouse monoclonal antibody–isotyping ELISA kit. The sensitivity of MELO mAb was estimated by establishing the indirect competition inhibition curve, and the half-maximal inhibitory concentration (**IC**; IC_{50}) was used to measure the sensitivity of the mAb, which was defined as the concentration of inhibitory substance when the ratio of the optical density (OD) value of the pore with the inhibitory substance to that of the control pore without the inhibitory substance was 50%. The linear range was equivalent to the range from IC_{20} to IC_{80}. The cross-reactivity of the MELO mAb with other NSAID of the oxicam group was investigated, and complete indirect competitive inhibition curves were conducted by ic-ELISA. The cross-reactivity rate was calculated according to the following formula:

$$\text{CR } (\%) = (IC_{50} \text{ of MELO})/(IC_{50} \text{ of other NSAID}) \times 100\%.$$

Preparation of mAb Labeled with Au Nanoparticles

Gold nanoparticles (**AuNP**) were synthesized according to a previously-described method (Chen et al., 2017; Wang et al., 2018a,b). In brief, 100 mL of chloroauric acid solution ($HAuCl_4$, 0.01%, wt/vol) was heated to boiling and continuously stirred for 15 min. Then, 2 mL of trisodium citrate solution (1%, wt/vol) was added and stirred. After the solution was heated for 15 min, the color of the solution turned to wine red. The solution was then cooled to room temperature and stored at 4°C until use.

The process of labeling the mAb with AuNP was as described in previous studies (Berlina et al., 2017; Guo et al., 2018). Briefly, the pH of 5 mL of AuNP solution was adjusted with 0.1 mol/L K_2CO_3. Then, 0.2 mL of mAb, adjusted to 0.1 mg/mL with borate buffer (0.02 mol/L), was added dropwise and incubated at room temperature for 40 min. Next, 1 mL of BSA solution (10%, wt/vol) was added to block the redundant free AuNP for 2 h at room temperature. After blocking, the mixture was centrifuged at 7,000 × *g* for 40 min (4°C) to remove unbound mAb, then the supernatant was discarded, and 1 mL of suspension buffer solution (0.02 mol/L pH 8.2 Tris containing 0.1% PEG, 0.1% Tween-20, 0.2% BSA, 5% sucrose, 5% trehalose, and 5% mannitol) was added. After resuspension, the redissolved AuNP-mAb was stored at 4°C until use.

Preparation and Test Procedure of ICS

As shown in Figure 3a, the ICS consisted of 4 parts: the sample pad, absorbent pad, nitrocellulose (**NC**) membrane, and polyvinyl chloride backing plate. The test (**T**) line and control (**CON**) line were both located on the NC membrane. The coating antigen (MELO hapten-OVA, 0.05 mg/mL) was bound on the T line, and the horseradish peroxidase (**HRP**)-labeled goat anti-mouse IgG (0.5 mg/mL) was bound on the CON line. The NC membrane was dried at 37°C and blocked with PBS [0.01 mol/L, containing 2% (wt/vol) BSA] at room temperature for 1 h. The sample pad was treated with PBS [0.01 mol/L, containing 1% (wt/vol) BSA, 0.2% (vol/vol) Tween-20, and 1% (wt/vol) sucrose] to promote the flow of sample solution and improve the stability of detection and dried at 37°C. The sample pad and absorbent pad were attached to the ends of the NC membrane with a 2-mm overlap with the NC membrane, and the polyvinyl chloride backing plate was located at the bottom of the strip.

To perform the test, 50 μL of AuNP-mAb and 150 μL of sample solution were added to 1 micropore and incubated for 5 min at room temperature. Then, the ICS was inserted into the micropore. Based on capillarity, the mixture solution flowed sequentially through the sample pad, T line, CON line, and absorbent pad. After 5 min, the test results could be observed by the naked eye. In negative samples, the AuNP-mAb was successively captured by the coating antigen on the T line and the HRP-labeled goat anti-mouse IgG on the CON line. The AuNP accumulated at the T line and the CON line, which turned red (Figure 3b). In a positive sample, the analyte primarily combined to the AuNP-mAb in the mixture solution. The AuNP-mAb that remained uncombined to analyte was captured by coating antigen on the T line. With the increasing analyte concentration, the color intensity of the T line became weaker. When the analyte concentration was enough to combine all the AuNP-mAb, the T line became colorless. Then, the dissociated AuNP-mAb was captured by the HRP-labeled goat anti-mouse IgG on the CON line, and the CON line turned red (Figure 3(b)).

Sample Pretreatment

The milk samples were purchased from a local supermarket and prepared for analysis. The fat and protein in milk affect the accuracy of the test results. Therefore,

in this study, extraction, centrifugation, and defatting were applied to reduce and eliminate the matrix effect. Briefly, 10 mL of milk was added into a 50-mL centrifuge tube, and the analyte was spiked. After oscillation, 20 mL of acetonitrile was added, and the mixture was vortexed for 2 min. Then, the mixture was centrifuged at 3,500 × *g* for 15 min at room temperature, and the residue was extracted again with acetonitrile. All of the supernatant was collected and dried with a gentle stream of nitrogen at 50°C. Subsequently, the extract was resolved in 2 mL of PBS (0.01 mol/mL, pH 7.4). Then, 2 mL of n-hexane was added into the extract, vortexed, and centrifuged at 3,500 × *g* for 10 min at room temperature. The n-hexane layer was discarded, and the subnatant was filtered through a 0.22-μm filter membrane for ICS and LC-MS/MS analysis.

RESULTS AND DISCUSSION

Characterization of Hapten

To fully expose the molecular structure of MELO, a spacer arm with carboxyl group was derived at the position of the hydroxyl to generate the MELO hapten. The LC-MS results are shown in Supplemental Figure S1 (https://doi.org/10.3168/jds.2020-19500). The chemical formula of the MELO hapten was $C_{18}H_{19}N_3O_6S_2$ and the exact mass was 437.07. For $[M-H]^-$, the m/z was 436.00. In addition, the molecular architecture of the MELO hapten was identified by nuclear magnetic resonance spectrometry (Supplemental Figure S2, https://doi.org/10.3168/jds.2020-19500). ^{1}H nuclear magnetic resonance (400 MHz, DMSO_d6): δ 14.80 (s, 1 H),

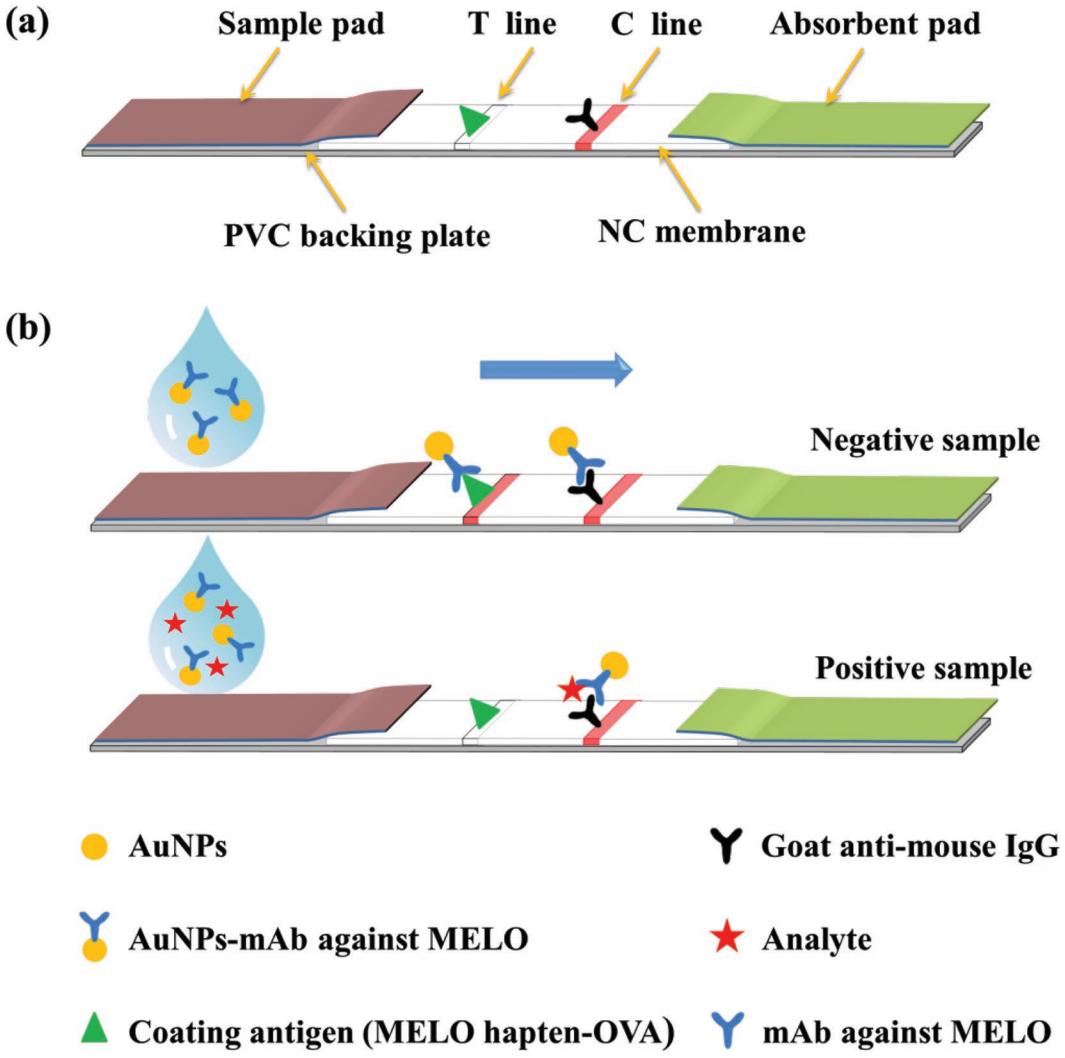

Figure 3. (a) Structure diagram of the immunochromatographic strip (ICS); (b) schematic diagram of ICS for nonsteroidal anti-inflammatory drug detection. T line = test line; C line = control line; PVC = polyvinyl chloride; NC = nitrocellulose; NP = nanoparticle; MELO = meloxicam; OVA = ovalbumin; mAb = monoclonal antibody.

8.03–8.05 (m, 1 H), 7.82–7.89 (m, 3 H), 7.45 (s, 1 H), 4.19–4.22 (m, 2 H), 2.91 (s, 3 H), 2.30–2.34 (m, 5 H), 2.03–2.06 (m, 2 H).

Characterization of Conjugates and mAb

The MELO hapten was conjugated to KLH as immunogen, and to OVA as coating antigen. All of the conjugations were characterized and analyzed with UV-visible spectroscopy. As shown in Supplemental Figure S3a (https://doi.org/10.3168/jds.2020-19500), the MELO hapten had 2 characteristic absorption peaks at 270 nm and 362 nm, and the KLH had 2 characteristic absorption peaks at 280 nm and 350 nm. The UV spectrum showed that the MELO hapten-KLH also had 2 characteristic absorption peaks, including the characteristic absorption peak of MELO hapten at 362 nm and a peak of MELO corresponding to KLH at 280 nm. Similarly, the characteristic absorption peaks of MELO hapten-OVA contained the peaks of MELO hapten at 362 nm and the peak of OVA at 280 nm Supplemental Figure S3b (https://doi.org/10.3168/jds.2020-19500). These confirmed that the immunogen MELO hapten-KLH and coating antigen MELO hapten-OVA were successfully synthetized.

Supplemental Figure S4a (https://doi.org/10.3168/jds.2020-19500) shows that the subclass of the mAb was mainly IgG. The IC_{50} and linear range of detection (IC_{20}–IC_{80}) were determined by the indirect competitive inhibition curve. As shown in Supplemental Figure S4b, the curve showed that the IC_{50} of the mAb against MELO was 0.31 ng/mL, and the IC_{20} to IC_{80} was in the range of 0.093 to 1.028 ng/mL. The cross-reactivity of the MELO mAb with other NSAID is shown in Table 1, and the complete indirect competitive inhibition curves are shown in Supplemental Figure S5 (https://doi.org/10.3168/jds.2020-19500). The IC_{50} values of the mAb were 0.49 ng/mL for LORN, 2.90 ng/mL for PIRO, 1.95 ng/mL for SUDO, 3.08 ng/mL for DRO, and 5.36 ng/mL for TENO. The linear ranges of detection were 0.134 to 1.756 ng/mL, 0.671 to 12.527 ng/mL, 0.404 to 9.410 ng/mL, 0.705 to 13.490 ng/mL, and 1.259 to 22.790 ng/mL, respectively. The results revealed that the mAb had high specificity for these 6 NSAID of the oxicam group. Consequently, the mAb could be used for the detection of MELO, LORN, PIRO, SUDO, DRO, and TENO.

Optimization of ICS

The pH of colloidal gold, the concentration of mAb, and the suspension buffer were optimized. The pH of colloidal gold was optimized by adding different volumes of K_2CO_3 (0.01 mol/L). It is generally believed that when the pH of colloidal gold is equal to the protein isoelectric point or slightly alkaline, the protein is electrically neutral. Therefore, the electrostatic interaction between the protein molecule and the colloidal gold is relatively small, and it is easy to adsorb the protein onto the surface of the colloidal gold. Protein molecules are firmly bound to the surface of colloidal gold to form a protein layer, which prevents the colloidal gold molecules from contacting each other and keeps the colloidal gold in a stable state. The concentration of mAb could affect the stability of colloidal gold and the visibility of ICS results. Colloidal gold will coagulate with an insufficient amount of mAb. The pH of colloidal gold was adjusted with 0.1 mol/L K_2CO_3 solution (4, 8, 12, and 16 μL), and a series of concentrations (10, 8, 6, and 4 μg/mL) of the mAb was used in the ICS. The AuNP-mAb was treated in suspension buffer solution mixed with 6 reagents (polyvinylpyrrolidone, PEG, BSA, Tween-20, Brij-30, and ON-870, each at concentrations of 5%). The results, based on the color intensity of the T line and CON line, indicated that the optimum volume of K_2CO_3 was 4 μL, the optimum concentration of mAb was 10 μg/mL, and the most stable color intensity of the T line was obtained with application of the surfactant Brij-30 (Supplemental Figure S6, https://doi.org/10.3168/jds.2020-19500).

Sensitivity Analysis of ICS

For qualitative detection, the sensitivity of ICS was evaluated by the cut-off value, which indicated the concentration of analyte when T line color disappeared. A visual limit of detection (**vLOD**) indicated the concentration of analyte at the beginning of the T line color change observed by the naked eye. A series of concentrations of 6 NSAID of the oxicam group were spiked into milk. After pretreatment, the final concentrations in milk were as follows: MELO (0, 0.1, 0.25, 0.5, 1, 2.5, and 5 ng/mL), LORN (0, 0.25, 0.5, 1, 2.5, and 5 ng/mL), PIRO (0, 0.5, 1, 2.5, 5, and 10 ng/mL), SUDO (0, 0.25, 0.5, 1, 2.5, 5, and 10 ng/mL), DRO (0, 1, 2.5, 5, 10, and 25 ng/mL), and TENO (0, 0.5, 1, 2.5, 5, 10, and 25 ng/mL). As shown in Figure 4, the results showed that the cut-off values in milk samples of these 6 NSAID were 5, 5, 10, 10, 25, and 25 ng/mL, respectively. The vLOD values in milk sample were 0.25, 1, 0.5, 0.5, 1, and 1 ng/mL, respectively. Therefore, concentrations of analyte in samples lower than the vLOD, between the vLOD and the cut-off value, and higher than the cut-off value, were considered to be negative, weakly positive, and positive, respectively.

Table 1. The cross-reactivity of meloxicam monoclonal antibody with other nonsteroidal anti-inflammatory drugs (NSAID)

NSAID	Structure	Half-maximal inhibitory concentration (ng/mL)	Cross reactivity (%)
Meloxicam	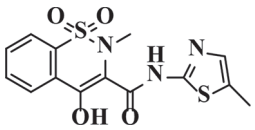	0.31	100
Lornoxicam	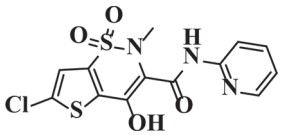	0.49	63.3
Piroxicam	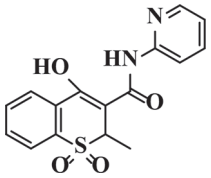	2.90	10.7
Sudoxicam	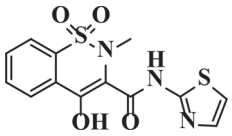	1.95	15.9
Droxicam	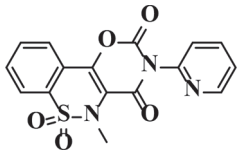	3.08	10.1
Tenoxicam	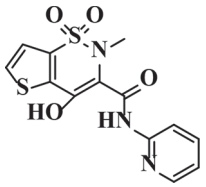	5.36	5.8

Sample Analysis by ICS and LC-MS/MS

Eighteen milk samples were analyzed using ICS and LC-MS/MS. None of the samples contained any of the 6 NSAID of the oxicam group. The analytes (MELO, LORN, PIRO, SUDO, DRO, and TENO) were spiked into milk samples with MELO (0, 5, and 10 ng/mL), LORN (0, 5, and 10 ng/mL), PIRO (0, 10, and 20 ng/mL), SUDO (0, 10, and 20 ng/mL), DRO (0, 20, and 30 ng/mL), and TENO (0, 20, and 30 ng/mL), respectively. As shown in Table 2, 18 milk samples were tested. It could be observed that the assay results of ICS were consistent with those of LC-MS/MS. Thus, the ICS is suitable for the detection of oxicam NSAID in milk samples.

CONCLUSIONS

In this study, a broad-spectrum mAb was successfully developed for the detection of 6 NSAID (MELO, LORN, PIRO, SUDO, DRO, and TENO) of the oxicam group. Based on this mAb, the immunochromatographic strip was developed, which could be used to test for the 6 NSAID of the oxicam group in a milk sample within 10 min. The cut-off values in milk samples of these 6 NSAID were 5, 5, 10, 10, 25, and 25 ng/mL, respectively. The vLOD values in milk samples were 0.25, 1, 0.5, 0.5, 1, and 1 ng/mL, respectively. After optimization, the test results of ICS corresponded well with those of LC-MS/MS. Our newly-developed ICS can be used for the detection of the 6 NSAID of the

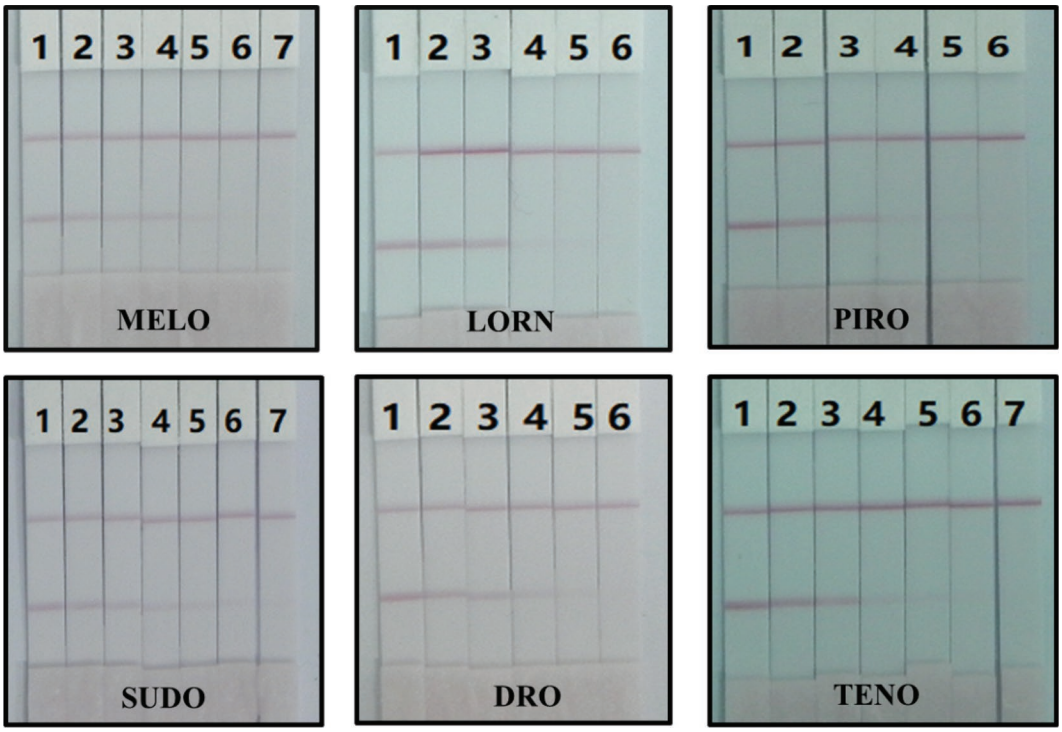

Figure 4. The detection results of 6 nonsteroidal anti-inflammatory drugs in milk samples by immunochromatographic strip. Concentrations of meloxicam (MELO): 1 = 0 ng/mL, 2 = 0.1 ng/mL, 3 = 0.25 ng/mL, 4 = 0.5 ng/mL, 5 = 1 ng/mL, 6 = 2.5 ng/mL, and 7 = 5 ng/mL. Concentrations of lornoxicam (LORN): 1 = 0 ng/mL, 2 = 0.25 ng/mL, 3 = 0.5 ng/mL, 4 = 1 ng/mL, 5 = 2.5 ng/mL, and 6 = 5 ng/mL. Concentrations of piroxicam (PIRO): 1 = 0 ng/mL, 2 = 0.5 ng/mL, 3 = 1 ng/mL, 4 = 2.5 ng/mL, 5 = 5 ng/mL, and 6 = 10 ng/mL. Concentrations of sudoxicam (SUDO): 1 = 0 ng/mL, 2 = 0.25 ng/mL, 3 = 0.5 ng/mL, 4 = 1 ng/mL, 5 = 2.5 ng/mL, 6 = 5 ng/mL, and 7 = 10 ng/mL. Concentrations of droxicam (DRO): 1 = 0 ng/mL, 2 = 1 ng/mL, 3 = 2.5 ng/mL, 4 = 5 ng/mL, 5 = 10 ng/mL, and 6 = 25 ng/mL. Concentrations of tenoxicam (TENO): 1 = 0 ng/mL, 2 = 0.5 ng/mL, 3 = 1 ng/mL, 4 = 2.5 ng/mL, 5 = 5 ng/mL, 6 = 10 ng/mL, and 7 = 25 ng/mL.

Table 2. Analysis of milk samples by immunochromatographic strip (ICS) and liquid chromatopgaphy–tandem mass spectrometry (LC-MS/MS)

Analyte	Spiked level (ng/mL)	ICS[1]	LC-MS/MS Measured ± SD (ng/mL)	Recovery (%)	Intraday CV (%)	Interday CV (%)
Meloxicam	0	ND	ND			
	5	+	4.28 ± 0.51	85.6	11.9	13.2
	10	++	10.18 ± 0.92	101.8	9.0	11.8
Lornoxicam	0	ND	ND			
	5	+	4.31 ± 0.49	86.2	11.4	12.6
	10	++	9.53 ± 0.93	95.3	9.8	11.7
Piroxicam	0	ND	ND			
	10	+	10.65 ± 0.97	106.5	9.1	12.5
	20	++	20.34 ± 2.25	101.7	11.2	13.6
Sudoxicam	0	ND	ND			
	10	+	10.32 ± 1.02	103.2	9.9	12.5
	20	++	20.11 ± 1.97	100.6	9.8	10.9
Droxicam	0	ND	ND			
	20	+	19.56 ± 2.04	97.8	10.4	11.6
	30	++	28.95 ± 3.31	96.5	11.4	13.3
Tenoxicam	0	ND	ND`			
	20	+	20.26 ± 1.87	101.3	9.2	12.3
	30	++	29.35 ± 2.95	97.8	10.0	13.4.

[1]ND = not detectable, the concentration of analyte was below visual limit of detection (vLOD); + = weak positive, the concentration of analyte was between vLOD and cut-off value; ++ = positive, the concentration of analyte exceeded the cut-off value.

oxicam group (MELO, LORN, PIRO, SUDO, DRO, and TENO) in high-throughput milk samples.

ACKNOWLEDGMENTS

This work was financially supported by National Key R&D Program (2019YFC1606603). The authors declare no competing financial interest.

REFERENCES

Barnette, D. A., M. A. Schleiff, L. R. Osborn, N. Flynn, M. Matlock, S. J. Swamidass, and G. P. Miller. 2020. Dual mechanisms suppress meloxicam bioactivation relative to sudoxicam. Toxicology 440:152478. https://doi.org/10.1016/j.tox.2020.152478.

Bartos, C., R. Ambrus, G. Katona, T. Sovany, R. Gaspar, A. Marki, E. Ducza, A. Ivanov, F. Tomosi, T. Janaky, and P. Szabo-Revesz. 2019. Transformation of meloxicam containing nanosuspension into surfactant-free solid compositions to increase the product stability and drug bioavailability for rapid analgesia. Drug Des. Devel. Ther. 13:4007–4020. https://doi.org/10.2147/DDDT.S220876.

Berlina, A. N., A. V. Zherdev, C. Xu, S. A. Eremin, and B. B. Dzantiev. 2017. Development of lateral flow immunoassay for rapid control and quantification of the presence of the colorant Sudan I in spices and seafood. Food Control 73:247–253. https://doi.org/10.1016/j.foodcont.2016.08.011.

Bertoni, G., A. Minuti, and E. Trevisi. 2015. Immune system, inflammation and nutrition in dairy cattle. Anim. Prod. Sci. 55:943. https://doi.org/10.1071/AN14863.

Bolarinwa, I. F., C. Orfila, and M. R. Morgan. 2014. Development and application of an enzyme-linked immunosorbent assay (ELISA) for the quantification of amygdalin, a cyanogenic glycoside, in food. J. Agric. Food Chem. 62:6299–6305. https://doi.org/10.1021/jf501978d.

Bradley, A. 2002. Bovine mastitis: An evolving disease. Vet. J. 164:116–128. https://doi.org/10.1053/tvjl.2002.0724.

Calvo, A. M., G. M. Santos, T. J. Dionisio, M. P. Marques, D. T. Brozoski, V. L. Lanchote, M. H. Fernandes, F. A. Faria, and C. F. Santos. 2016. Quantification of piroxicam and 5′-hydroxypiroxicam in human plasma and saliva using liquid chromatography-tandem mass spectrometry following oral administration. J. Pharm. Biomed. Anal. 120:212–220. https://doi.org/10.1016/j.jpba.2015.12.042.

Chen, Y., L. Guo, L. Liu, S. Song, H. Kuang, and C. Xu. 2017. Ultrasensitive immunochromatographic strip for fast screening of 27 sulfonamides in honey and pork liver samples based on a monoclonal antibody. J. Agric. Food Chem. 65:8248–8255. https://doi.org/10.1021/acs.jafc.7b03190.

Colditz, I. G., D. R. Paull, J. B. Lloyd, L. Johnston, and A. H. Small. 2019. Efficacy of meloxicam in a pain model in sheep. Aust. Vet. J. 97:23–32. https://doi.org/10.1111/avj.12779.

Cox, S., J. Hayes, J. Yarbrough, T. Veiga-Parga, and C. Greenacre. 2014. High-performance liquid chromatography determination of meloxicam and piroxicam with ultraviolet detection. Chromatogr. Res. Int. 2014:1–7. https://doi.org/10.1155/2014/521697.

Dong, G., Y. Pan, Y. Wang, S. Ahmed, Z. Liu, D. Peng, and Z. Yuan. 2018. Preparation of a broad-spectrum anti-zearalenone and its primary analogues antibody and its application in an indirect competitive enzyme-linked immunosorbent assay. Food Chem. 247:8–15. https://doi.org/10.1016/j.foodchem.2017.12.016.

Dowling, G., and E. Malone. 2011. Analytical strategy for the confirmatory analysis of the non-steroidal anti-inflammatory drugs firocoxib, propyphenazone, ramifenazone and piroxicam in bovine plasma by liquid chromatography tandem mass spectrometry. J. Pharm. Biomed. Anal. 56:359–365. https://doi.org/10.1016/j.jpba.2011.05.029.

Emara, L., M. Emam, N. Taha, H. Raslan, and A. El-Ashmawy. 2016. A simple and sensitive HPLC/UV method for determination of meloxicam in human plasma for bioavailability and bioequivalence studies. J. App. Pharm. Sci. 6:012–019. https://doi.org/10.7324/japs.2016.60702.

Fang, B., S. Hu, C. Wang, M. Yuan, Z. Huang, K. Xing, D. Liu, J. Peng, and W. Lai. 2019. Lateral flow immunoassays combining enrichment and colorimetry-fluorescence quantitative detection of sulfamethazine in milk based on trifunctional magnetic nanobeads. Food Control 98:268–273. https://doi.org/10.1016/j.foodcont.2018.11.039.

Guo, L., X. Wu, L. Liu, H. Kuang, and C. Xu. 2018. Gold nanoparticle-based paper sensor for simultaneous detection of 11 benzimidazoles by one monoclonal antibody. Small 14:1701782. https://doi.org/10.1002/smll.201701782.

Guo, S., Y. Cui, K. Wang, W. Zhang, G. Tan, B. Wang, and L. Cui. 2016. Development of a specific monoclonal antibody for the quantification of artemisinin in artemisia annua and rat serum. Anal. Chem. 88:2701–2706. https://doi.org/10.1021/acs.analchem.5b04058.

Hua, X., X. Liu, W. Yin, Y. Xia, Q. Zhou, Y. Lu, W. Li, H. Shi, F. Liu, and M. Wang. 2015. A sensitive monoclonal antibody-based enzyme-linked immunosorbent assay for the detection of bifenthrin in a chemical soil barrier. Sci. Total Environ. 502:246–251. https://doi.org/10.1016/j.scitotenv.2014.09.032.

Kazemi, M., R. Mombeiny, S. Tavakol, P. Keyhanvar, and K. Mousavizadeh. 2019. A combination therapy of nanoethosomal piroxicam formulation along with iontophoresis as an anti-inflammatory transdermal delivery system for wound healing. Int. Wound J. 16:1144–1152. https://doi.org/10.1111/iwj.13171.

Kimble, B., K. M. Li, and M. Govendir. 2013. Quantitation of meloxicam in the plasma of koalas (*Phascolarctos cinereus*) by improved high performance liquid chromatography. J. Vet. Sci. 14:7–14. https://doi.org/10.4142/jvs.2013.14.1.7.

Liu, A., J. Lin, M. Dai, B. Ma, Y. Wu, J. Fang, and M. Zhang. 2016. Development of a Monoclonal Antibody-Based Immunochromatographic Assay Detecting Ractopamine Residues in Swine Urine. Food Anal. Methods 9:2016–2025. https://doi.org/10.1007/s12161-015-0382-5.

Majdinasab, M., M. Zareian, Q. Zhang, and P. Li. 2019. Development of a new format of competitive immunochromatographic assay using secondary antibody-europium nanoparticle conjugates for ultrasensitive and quantitative determination of ochratoxin A. Food Chem. 275:721–729. https://doi.org/10.1016/j.foodchem.2018.09.112.

Newby, N. C., D. L. Pearl, S. J. Leblanc, K. E. Leslie, M. A. von Keyserlingk, and T. F. Duffield. 2013. Effects of meloxicam on milk production, behavior, and feed intake in dairy cows following assisted calving. J. Dairy Sci. 96:3682–3688. https://doi.org/10.3168/jds.2012-6214.

Newby, N. C., D. R. Tremblay, and T. F. Duffield. 2014. Evaluation of the effects of treating dairy cows with meloxicam at calving on retained fetal membranes risk. Can. Vet. J. 55:1196–1199.

Olson, M. E., B. Ralston, L. Burwash, H. Matheson-Bird, and N. D. Allan. 2016. Efficacy of oral meloxicam suspension for prevention of pain and inflammation following band and surgical castration in calves. BMC Vet. Res. 12:102. https://doi.org/10.1186/s12917-016-0735-3.

Pascottini, O. B., M. R. Carvalho, S. J. Van Schyndel, E. Ticiani, J. W. Spricigo, L. K. Mamedova, E. S. Ribeiro, and S. J. LeBlanc. 2019. Feed restriction to induce and meloxicam to mitigate potential systemic inflammation in dairy cows before calving. J. Dairy Sci. 102:9285–9297. https://doi.org/10.3168/jds.2019-16558.

Rúbies, A., L. Guo, F. Centrich, and M. Granados. 2016. Analysis of non-steroidal anti-inflammatory drugs in milk using QuEChERS and liquid chromatography coupled to mass spectrometry: Triple quadrupole versus Q-Orbitrap mass analyzers. Anal. Bioanal. Chem. 408:5769–5778. https://doi.org/10.1007/s00216-016-9679-5.

Shirako, J., M. Kawasaki, K. Komine, Y. Kunisue, M. Terada, C. Sasaki, W. Irie, C. Murakami, K. Tonooka, K. Tomobe, and T. Shinozuka. 2013. Simultaneous determination for oxicam non-steroidal anti-inflammatory drugs in human serum by liquid chromatog-

raphy-tandem mass spectrometry. Forensic Sci. Int. 227:100–102. https://doi.org/10.1016/j.forsciint.2012.11.016.

Shock, D., S. Roche, and M. Olson. 2019. A comparative pharmacokinetic analysis of oral and subcutaneous meloxicam administered to postpartum dairy cows. Vet. Sci. 6:73. https://doi.org/10.3390/vetsci6030073.

Swartz, T. H., H. H. Schramm, J. M. Bewley, C. M. Wood, K. E. Leslie, and C. S. Petersson-Wolfe. 2018. Meloxicam administration either prior to or after parturition: Effects on behavior, health, and production in dairy cows. J. Dairy Sci. 101:10151–10167. https://doi.org/10.3168/jds.2018-14657.

Wang, Z., L. Guo, L. Liu, H. Kuang, and C. Xu. 2018b. Colloidal gold-based immunochromatographic strip assay for the rapid detection of three natural estrogens in milk. Food Chem. 259:122–129. https://doi.org/10.1016/j.foodchem.2018.03.087.

Wang, S., M. Jiang, Z. Ju, X. Qiao, and Z. Xu. 2018a. A flow-injection chemiluminescent biomimetic immunoassay method using a molecularly imprinted polymer as a biomimetic antibody for the determination of trichlorfon. Food Agric. Immunol. 29:159–170. https://doi.org/10.1080/09540105.2017.1364707.

Wang, C., X. Li, T. Peng, Z. Wang, K. Wen, and H. Jiang. 2017. Latex bead and colloidal gold applied in a multiplex immunochromatographic assay for high-throughput detection of three classes of antibiotic residues in milk. Food Control 77:1–7. https://doi.org/10.1016/j.foodcont.2017.01.016.

Wang, Z., T. Mi, R. C. Beier, H. Zhang, Y. Sheng, W. Shi, S. Zhang, and J. Shen. 2015. Hapten synthesis, monoclonal antibody production and development of a competitive indirect enzyme-linked immunosorbent assay for erythromycin in milk. Food Chem. 171:98–107. https://doi.org/10.1016/j.foodchem.2014.08.104.

Wang, F., H. Wang, Y. D. Shen, Y. J. Li, J. X. Dong, Z. L. Xu, J. Y. Yang, Y. M. Sun, and Z. L. Xiao. 2016. Bispecific monoclonal antibody-based multianalyte ELISA for furaltadone metabolite, malachite green, and leucomalachite green in aquatic products. J. Agric. Food Chem. 64:8054–8061. https://doi.org/10.1021/acs.jafc.6b03233.

Wang, Y., J. Xu, Y. Qiu, P. Li, B. Liu, L. Yang, B. Barnych, B. D. Hammock, and C. Zhang. 2019. Highly specific monoclonal antibody and sensitive quantum dot beads-based fluorescence immunochromatographic test strip for tebuconazole assay in agricultural products. J. Agric. Food Chem. 67:9096–9103. https://doi.org/10.1021/acs.jafc.9b02832.

Woodland, A. N., D. Van der Saag, B. Kimble, P. J. White, M. Govendir, and S. Lomax. 2019. Plasma pharmacokinetic profile and efficacy of meloxicam administered subcutaneously and intramuscularly to sheep. PLoS One 14:e0215842. https://doi.org/10.1371/journal.pone.0215842.

You, J., C. Wu, and X. Wang. 2018. The thermal decomposition mechanism and kinetics of tenoxicam. J. Anal. Appl. Pyrolysis 134:573–579. https://doi.org/10.1016/j.jaap.2018.08.006.

Zangaro, G. A. C., A. C. S. Carvalho, B. Ekawa, A. L. C. S. do Nascimento, W. D. G. Nunes, R. P. Fernandes, G. M. B. Parkes, G. P. Ashton, M. Ionashiro, and F. J. Caires. 2019. Study of the thermal behavior in oxidative and pyrolysis conditions of some transition metals complexes with lornoxicam as ligand using the techniques: TG-DSC, DSC, HSM and EGA (TG-FTIR and HSM-MS). Thermochim. Acta 681:178399. https://doi.org/10.1016/j.tca.2019.178399.

ORCIDS

Chuanlai Xu https://orcid.org/0000-0002-5639-7102